

# A 2-D Active Appearance Model For Prostate Segmentation in Ultrasound Images

R. Medina<sup>\*</sup>, A. Bravo<sup>†</sup>, P. Windyga<sup>§</sup>, J. Toro<sup>‡</sup>, P. Yan<sup>§</sup> and G. Onik<sup>¶</sup>

<sup>\*</sup>Universidad de Los Andes, Grupo de Ingeniería Biomédica (GIBULA)  
Mérida 5101, Venezuela  
Email: rmedina@ula.ve

<sup>†</sup>Universidad Experimental del Táchira, Grupo de Ingeniería Biomédica  
San Cristobal 5001, Venezuela

<sup>§</sup>School of Computer Science, University of Central Florida, Orlando, Florida, USA

<sup>‡</sup>Département d'Informatique, Université de Sherbrooke, Sherbrooke (Quebec), Canada J1K 2R1

<sup>¶</sup>Center for Surgical Advancement, Florida Hospital Celebration Health, Celebration, Florida, USA

**Abstract**—In this research we use an active appearance model (AAM) as the core of a robust segmentation algorithm that combines contour and texture information to learn shape variability through a training procedure in trans-rectal ultrasound (TRUS) images of the prostate. Training was carried out using a dataset of 95 images which are preprocessed using gray-level mathematical morphology operators. Preliminary results are promising. The segmentation can provide shapes that have an overlap with respect to a ground truth shape, traced by an expert, of up to 96%, and an average distance from point to curve of up to 1.3 pixels.

## I. INTRODUCTION

Prostate cancer is a major health concern among men age 50 and older [1]. Since 1980, the incidence of prostate cancer has risen steadily to become the second most common cause of cancer-related deaths among men, exceeded only by lung cancer [2]. Yet, the disease is curable if detected early.

Prostate cancer has long been a quiet killer in part because it is often asymptomatic until it has reached an advanced stage and because, until recent years, the topic has been absent from public discourse. As awareness of this life-threatening disease has grown, demand for improved treatment alternatives has increased. Several treatment options for prostate cancer exist, ranging from radiation therapy to prostate removal. In recent years, percutaneous targeted prostate ablation has emerged as a treatment option for the patients seeking a minimally invasive alternative to radiation therapy. The technique has evolved considerably since first attempted in the 1960s. It is now a one- to two-hour minimally invasive surgical procedure that enables physicians to precisely freeze and destroy cancerous tissue in the prostate gland without damaging surrounding healthy tissue. Accurate monitoring and control of the procedure is currently achieved by employing both intra-operative ultrasound (US) and temperature monitoring [3].

Although a marked increase in the utilization of the procedure has been observed, the current number of surgeons capable of performing targeted cryosurgery safely and effectively is quite low. Nevertheless, this situation may be improved. Prostate surgeons who carry out cryosurgical procedures may

be trained by using Virtual Reality (VR) based tools. All these tools rely on realistic anatomical models that should be extracted from multimodal imaging techniques. In procuring a model, segmentation is a key preliminary task no matter which imaging modality is chosen [2].

Ultrasound (US) images are the preferred imaging modality for prostate diagnosis and treatment [4]. Trans-rectal ultrasound (TRUS) provides 2-D or 3-D images of the prostate gland without overlapping of other anatomical structures. For any application, such as prostate volume measurement or cryosurgery, an accurate detection of the prostate contour is necessary. A problem, however, is that detection of the prostate's contour is a difficult task due to poor contrast between the tissues, speckle noise, shadowing and refraction artifacts [5]. In clinical routines, manual contouring is a simple approach that is usually performed by experienced medical staff. Yet, this kind of segmentation is subjective and tedious. These limitations have motivated the development of semi-automatic or automatic contour detection algorithms. Several algorithms have been proposed. They have been classified as edge-, texture- and model-based detection methods [5]. In edge-based detection methods, the idea is to find the edges in the image and then to select and link the more plausible edges that could correspond to the prostate boundary. These approaches can only work in well contrasted images where the prostate boundary is clearly defined. Examples of these approaches are [6] and [7]. Texture-based methods detect the prostate contour as regions in the image with different measures of texture [8]. Texture- and edge-based methods are rather inaccurate for prostate contour detection. In contrast, model-based contour detection methods are more efficient and have recently motivated important research aimed at enhancing the performance of such approaches. These methods integrate prior information about the object together with features extracted from the image to build a model useful for contour detection [9]–[11].

Deformable models have been widely used for segmentation of images resulting from different imaging modalities. Despite their widespread use, these methods are sensible to

initialization and sometimes they are not able to detect the object contour and require user intervention. Recently, in [12], [13] an active shape model is used for segmenting the prostate shape in abdominal ultrasound images. The performance of these approaches is promising, however, the texture information is not exploited. Aiming at solving this limitation, Cootes *et al.* [14] introduced the Active Appearance Model (AAM) that integrates a statistical model of shape with texture information. AAM algorithms have been successfully used for segmentation of cardiac Magnetic Resonance (MR) and ultrasound images [15]. In this paper, we show results on the segmentation of TRUS prostate images using AAM.

## II. METHODS

### A. Background in AAM

The segmentation procedure using AAM involves two stages. In the first stage a training procedure is performed based on a set of landmarks describing planar shapes. The second stage corresponds to the segmentation where the Active Appearance Model is perturbed (by varying some of their parameters) in order to generate instances of the model matching the contour and gray-level information in the image [14]. In both stages, each planar shape is represented by  $n$  points as the vector:

$$\mathbf{x} = [x_1, x_2, \dots, x_n; y_1, y_2, \dots, y_n]^T. \quad (1)$$

This is an observation in the  $2n$  dimensional space. Principal Component Analysis (PCA) is used for dealing with redundancy in the input data after alignment using the procrustes analysis [16]. The resulting shape model is a function of the mean shape  $\bar{\mathbf{x}}$ , a matrix  $\Phi_s$  which includes the eigenvectors of the covariance matrix of the input data, and a set of parameters  $\mathbf{b}_s$  according to:

$$\mathbf{x} = \bar{\mathbf{x}} + \Phi_s \mathbf{b}_s. \quad (2)$$

The points of the shape are transformed into a modal representation where the modes are ordered according to the percentage of variation that they explain. The gray-level information is also modeled as a texture-model where pixel intensities after normalization are considered. For  $m$  samples over the object, the texture is represented as the vector:

$$\mathbf{g}_m = [g_1, g_2, \dots, g_m]^T. \quad (3)$$

The texture inside the shape is sampled using a piecewise affine warp based on the Delaunay triangulation of the mean shape. A normalization of the texture information is performed and then PCA yields the following representation:

$$\mathbf{g} = \bar{\mathbf{g}} + \Phi_g \mathbf{b}_g, \quad (4)$$

where  $\bar{\mathbf{g}}$  is the mean texture,  $\Phi_g$  includes the eigenvectors of the covariance matrix and  $\mathbf{b}_g$  is the set of deformation parameters. The combined formulation leads to the appearance model. As there are correlations between the shape and

texture variations, a concatenated vector is generated as:

$$\mathbf{b} = \begin{pmatrix} \mathbf{W}_s \mathbf{b}_s \\ \mathbf{b}_g \end{pmatrix} = \begin{pmatrix} \mathbf{W}_s \Phi_s^T (\mathbf{x} - \bar{\mathbf{x}}) \\ \Phi_g^T (\mathbf{g} - \bar{\mathbf{g}}) \end{pmatrix}, \quad (5)$$

where  $\mathbf{W}_s$  is a diagonal matrix whose entries are the weighting parameters that account for the differences of units between shape (distances) and gray-level models (pixel intensities) [17]. A third PCA is applied to this vector leading to the combined model:

$$\mathbf{b} = \mathbf{Q} \mathbf{c}, \quad (6)$$

where  $\mathbf{Q}$  is a matrix of eigenvectors and  $\mathbf{c}$  is a vector of appearance parameters controlling both shape and gray-level of the model. Shape and texture can then be synthesized from the model in equation (5) as:

$$\begin{aligned} \mathbf{x} &= \bar{\mathbf{x}} + \Phi_s \mathbf{W}_s^{-1} \mathbf{Q}_s \mathbf{c}, \\ \mathbf{g} &= \bar{\mathbf{g}} + \Phi_g \mathbf{Q}_g \mathbf{c}. \end{aligned} \quad (7)$$

To use this AAM for segmentation requires an optimization process where the differences between the input image and the one synthesized by the model are minimized.

### B. Preprocessing

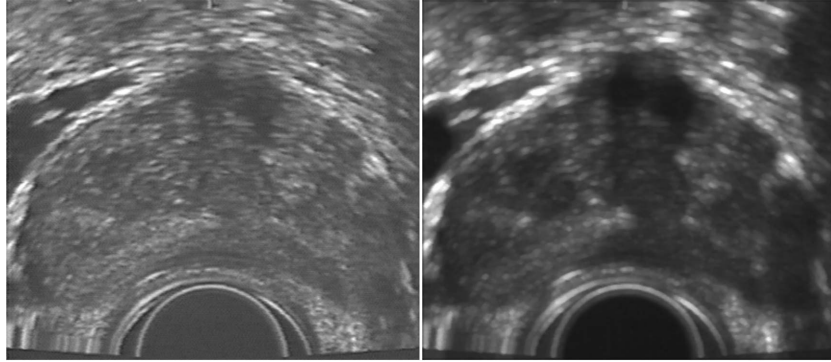
The ultrasound images are first preprocessed using a median filter of size  $3 \times 3$  to obtain image  $I_1$ . This image is subsequently processed using a gray-level morphology operator corresponding to a dilation with a disk shaped structure element with radius equal to 12 pixels. The dilated image is then processed with a closing and a eroding operator using a disk shaped structure element with radius equal to 6 pixels. The resulting image is smoothed using a Gaussian filter of size  $5 \times 5$  and standard deviation of 1.5 to obtain image  $I_2$ . Images  $I_1$  and  $I_2$  are multiplied and the result is then re-scaled to obtain the final preprocessed image that is used for segmentation. Figure 1(a) shows the original image and Figure 1(b) shows the preprocessed image.

### C. Training procedure

In the training procedure several tasks are performed. The first task is the manual tracing, by a medical expert, of a set of points located in each prostate contour. As for the AAM algorithm, a set of landmarks is required that should be in correspondence within the population of shapes. The algorithm proposed by Hill *et al.* [18] for automatic landmark identification is used. A set of 95 images is considered as a training set and 51 landmark points are used in each image for modeling the prostate shape. Combination of shape variability and texture variability after using PCA on the combined information leads to a compact appearance model that is used for performing a robust segmentation.

### D. Segmentation

Segmentation is carried out as an optimization procedure where the difference between the synthesized object obtained from AAM and the actual image is minimized. An iterative algorithm is used for the optimization. At each iteration, a controlled perturbation of the parameters of the model is



(a) (b)  
Fig. 1. a) Original image, b) Preprocessed image.

introduced in order to approach the target prostate shape. By adjusting the combined model parameters and pose (which defines the position, size and orientation of the shape), the texture mode,  $g_{model}$ , can be deformed to fit the image texture,  $g_{image}$ , by minimizing the square error:

$$E = \sum_{i=1}^m (g_{model}(i) - g_{image}(i))^2 = \sum_{i=1}^m (\delta g_i)^2 = \|\delta \mathbf{g}\|^2. \quad (8)$$

Since the model has many parameters, this is a difficult optimization problem [14]. The optimization is usually performed under the assumption of a linear relationship between parameters change  $\delta \mathbf{c}$  and pixel differences  $\delta \mathbf{g}$ ,

$$\delta \mathbf{c} = \mathbf{R} \delta \mathbf{g}. \quad (9)$$

Matrix  $\mathbf{R}$  is determined from a set of 24,474 experiments on the training set. This set of experiments is fed into a multivariate linear regression framework. Each experiment consists in displacing the model parameters  $\mathbf{c}$  and the pose parameters  $\mathbf{t}$  by a known amount and measuring the difference between the texture described by the model and the actual texture in the image located at the corresponding pixels (see [16] for details). The pose parameters are given by:

$$\mathbf{t} = (s_x, s_y, t_x, t_y)^T, \quad (10)$$

where  $s_x = s \cos(\theta) - 1$  and  $s_y = s \sin(\theta)$  are the combined scaling and rotation with  $\theta$  being the rotation and  $s$  the scale parameter; additionally,  $t_x$  and  $t_y$  are the translation parameters.

### III. RESULTS

A set of 95 TRUS trans-axial images of the prostate is considered. Each image is quantized with 8 bits per pixel and the size is  $640 \times 480$  pixels. Figure 1 shows one of the images in the set before and after preprocessing. The training and segmentation of images was performed using the Application Interface (API) developed by Stegman *et al.* [16] from the IMM at The Technical University of Denmark. The training procedure is performed on the images in the set using the leave-one out method where each training example is missing out in turn and evaluated upon. In Figure 2(a),

the shape model obtained after training is shown overlaid on image 29 of the test set. The model is located in a position that is only an approximation of the actual prostate contour. Notice that the model is far from the actual contour in the left portion of the image. In Figure 2(b), the model is shown after segmentation. The procedure takes 14 iterations for attaining convergence. The area overlap of the final contour with respect to the ground truth contour is 96% and the average point to curve distance (Pt.Crv) is 1.3 pixels. A preliminary evaluation of the method in ultrasound prostate images, using the leave-one out method, is performed using the set of 95 images. Segmentation is performed in the excluded image using four different automatically generated initializations. The solution that gives the lower Pt.Crv distance is retained. The average point to curve distance (mean  $\pm$  standard deviation) is  $3.58 \pm 1.49$  pixels with a minimum of 1.3 pixels and a maximum of 8.92 pixels. This is close to results obtained in [12] and [13] where the mean distance is 3.2 pixels. They, however, consider a small set of images (8 images in [12] and 10 in [13]) and do not provide any other indication of the tendency of measured Pt.Crv distances. An additional test on an image of the prostate close to the apex, where segmentation is difficult even for the trained expert, is shown in Figure 3. In this case, the average point to curve distance is 8.92 pixels. Note, though, that the algorithm converges to a plausible contour compatible with the gray-level information, even when the image is characterized by low contrast and low signal-to-noise ratio. The differences may be explained by the fact that the expert tries to draw in this region the subjective contour that would correspond to the prostate.

### IV. CONCLUSIONS

A robust method for prostate segmentation was proposed that is able to cope with imperfections related to the ultrasound imaging modality. The active appearance model codes the variability in shape and in texture during the training procedure leading to a compact representation. The appearance of this model is deformed during the segmentation procedure in order to match the target objects in the image. First results on TRUS images are promising, however, further research on

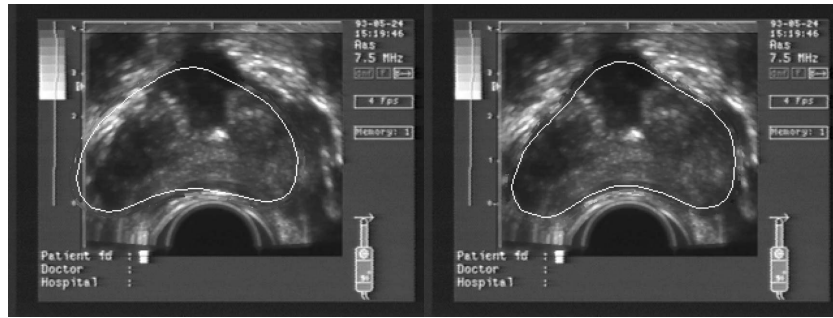


Fig. 2. a) Initial position of the active appearance model, b) Model fitted to the prostate using AAM.

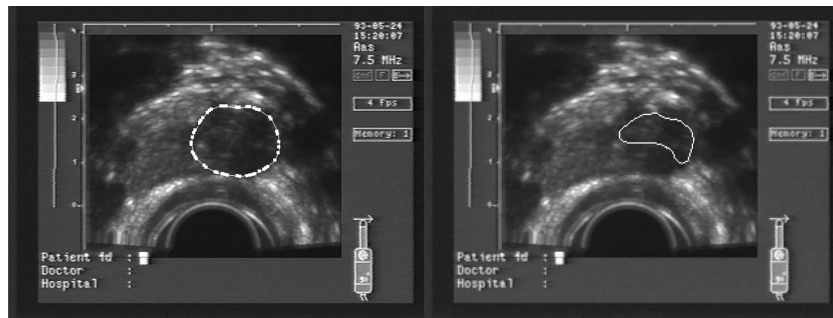


Fig. 3. a) Manually traced contour of the prostate, b) Model fitted to the prostate using AAM.

methods to improve the convergence of the model is required. A complete validation including comparison to other existent methods is also part of the future work in this subject.

#### ACKNOWLEDGMENT

The authors would like to thank the Investigation Dean's Office of Universidad Nacional Experimental del Táchira, the CDCHT from Universidad de Los Andes, and the University Sector Planning Office (OPSU) through its Program Alma Mater for their support to this project.

#### REFERENCES

- [1] J. Corrigan, J. W. Jacobson, *et al.*, "Prostate cancer progress report," National Cancer Institute, New York, U.S.A, Tech. Rep., 2004.
- [2] P. Windyga, G. Onik, and R. Medina, "Virtual trainer for prostate cryosurgery," in *Proceedings of the IASTED conference in Modeling System*, San Diego, CA, USA, 2003, pp. 229–233.
- [3] G. M. Onik, D. B. Downey, and A. Fenster, "Three-dimensional sonographically monitored cryosurgery in a prostate phantom," *Journal of Ultrasound Medicine*, no. 15, pp. 267–270, 1996.
- [4] A. Fenster and D. Downey, "Three-dimensional ultrasound imaging," in *Proceedings of SPIE: Medical Physics.*, San Diego, CA, USA, 1999, pp. 2–11.
- [5] F. Shao, K. V. Ling, W. S. Ng, and R. Y. Wu, "Prostate boundary detection from ultrasonographic images," *Journal of Ultrasound in Medicine*, vol. 22, pp. 605–623, 2003.
- [6] Y. J. Liu, W. S. Ng, M. Y. Teo, and H. C. Lim, "Computerized prostate boundary estimation in ultrasound images using the radial bas-relief method," *Medical and Biological Engineering and Computing*, vol. 35, pp. 4450–4454, 1997.
- [7] R. G. Aarnink, S. D. Pathak, J. J. de la Rosette, F. M. J. Debruyne, Y. Kim, and H. Wijkstra, "Edge detection in prostatic ultrasound images using integrated edge maps," *Ultrasonics*, vol. 36, pp. 637–644, 1998.
- [8] W. D. Richard and C. G. Keen, "Automated texture-based segmentation of ultrasound images of the prostate," *Computerized Medical Imaging and Graphics*, vol. 20, pp. 131–140, 1996.
- [9] P. Abolmaesumi and M. R. Sirouspour, "Segmentation of prostate contours from ultrasound images," in *2004 IEEE International Conference on Acoustics Speech and Signal Processing (ICASSP'2004)*, vol. III, Montreal, Canada, 2004, pp. 517–520.
- [10] S. D. Pathak, R. G. Aarnink, J. de la Rosette, V. Chalana, H. Wijkstra, F. M. J. Debruyne, and Y. Kim, "Quantitative three-dimensional trans-rectal ultrasound for prostate imaging," in *Proceedings of SPIE-Medical Imaging 1998: Image Display*, vol. 3335, 1998, pp. 83–92.
- [11] H. M. Ladak, F. Mao, Y. Wang, D. B. Downey, D. A. Steinman, and A. Fenster, "Prostate boundary segmentation from 2d ultrasound images," *Medical Physics*, vol. 27, pp. 1777–1788, 2000.
- [12] D. Shen, Y. Zhan, and C. Davatzikos, "Segmentation of prostate boundaries from ultrasound images using statistical shape model," *IEEE Transactions on Medical Imaging*, vol. 22, pp. 539–551, 2003.
- [13] N. Betrouni, M. Vermandel, D. Pasquier, S. Maouche, and J. Rousseau, "Segmentation of abdominal ultrasound images of the prostate using a priori information and an adapted noise filter," *Computerized Medical Imaging and Graphics*, vol. 29, pp. 43–51, 2005.
- [14] T. F. Cootes, G. J. Edwards, and C. J. Taylor, "Active appearance models," in *Proceedings of The European Conference in Computer Vision*, vol. 2, 1998, pp. 484–498.
- [15] S. C. Mitchell, J. G. Bosch, B. P. F. Lelieveldt, R. J. van der Geest, J. H. C. Reiber, and M. Sonka, "3-d active appearance models: Segmentation of cardiac mr and ultrasound images," *IEEE Transactions on Medical Imaging*, vol. 21, pp. 1167–1178, 2002.
- [16] M. B. Stegmann, B. K. Ersboll, and R. Larsen, "FAME: A flexible appearance modeling environment," *IEEE Transactions on Medical Imaging*, vol. 22, no. 10, pp. 1319–1331, 2003.
- [17] T. F. Cootes and C. J. Taylor, "Statistical models of appearance for computer vision," University of Manchester, Wolfson Image Analysis Unit, Tech. Rep., 2001.
- [18] A. Hill, C. J. Taylor, and A. D. Brett, "A framework for automatic landmark identification using a new method of nonrigid correspondence," *IEEE Transactions on Pattern Analysis and Machine Intelligence*, vol. 22, no. 3, pp. 241–251, 2000.